nature materials

REVIEW ARTICLE

PUBLISHED ONLINE: 23 APRIL 2010 | DOI: 10.1038/NMAT2743

Transformation optics and metamaterials

Huanyang Chen[1*], C. T. Chan[2] and Ping Sheng[2]

Underpinned by the advent of metamaterials, transformation optics offers great versatility for controlling electromagnetic waves to create materials with specially designed properties. Here we review the potential of transformation optics to create functionalities in which the optical properties can be designed almost at will. This approach can be used to engineer various optical illusion effects, such as the invisibility cloak.

A spatially changing refractive index leads to changes in light-propagation characteristics. The most common example is a lens, which is a curved piece of glass that bends light as the light experiences a single change of refractive index through the air/glass interface. A medium with a continuously changing refractive index can bend light to create amazing illusion effects, such as the mirage effect in deserts. Recently it was realized that artificial media that have spatially changing optical properties can bend light in almost any manner. The most remarkable example is the so-called invisibility cloak[1,2] that can steer light around an object to make it seem invisible. The mathematical technique that enables us to design such artificial materials is called transformation optics[1,2]. Initially driven by the possibility of realizing the invisibility cloak, transformation optics has now evolved into a powerful tool for designing a wide variety of new optical effects and devices, some of which have already been created, whereas others are possible with the aid of metamaterials.

To understand how transformation optics works, let us consider light propagation over a small distance Δx in a material with refractive index η. The phase change in that distance is given by $(\omega/c)\eta\Delta x$, where ω is the angular frequency and c is the speed of light. We can alternatively write the phase change as $(\omega/c)\Delta x'$, where $\Delta x' = \eta\Delta x$ represents a scale change that preserves the phase of the light and hence its propagation characteristics. Now suppose that η is a function of the spatial coordinate, that is, $\eta(\mathbf{x})$. Then changes in scale, or local transformations, can occur everywhere. Such a correspondence between materials parameters (refractive index) and the coordinate system can become useful if it is reformulated in a mathematically rigorous manner. For example, it is shown[3] that two-dimensional (2D) electromagnetic problems with complex geometries (say a curved wave guide) can be solved by performing a conformal mapping of coordinates so that the geometry becomes simple (say a straight wave guide), while the refractive index profile is changed to a more complex profile, with the refractive index at each point changed by a scale factor that is the ratio of the differential lengths of the two sets of coordinates. In this way a coordinate transformation results in a new $\eta(\mathbf{x})$. Such correspondence between materials and coordinate transformation is a special property of Maxwell's equations that govern the propagation of light: these equations maintain the same form (so-called form invariance) under a coordinate transformation[4–10] and thereby guarantee the physical character of light propagation to be upheld at the differential scale. This characteristic is the basis of transformation optics.

In general, Maxwell's equations at a fixed frequency can be written as[8]:

$$\nabla \times \mathbf{E} + i\omega\mu\mathbf{H} = 0, \nabla \times \mathbf{H} - i\omega\varepsilon\mathbf{E} = 0$$

If a coordinate transformation $x' = x'(\mathbf{x})$ is applied, the equations maintain the same form[8] in the transformed coordinate system

$$\nabla \times \mathbf{E}' + i\omega\mu'\mathbf{H}' = 0, \nabla \times \mathbf{H}' - i\omega\varepsilon'\mathbf{E}' = 0$$

The permittivity tensor (ε') and permeability tensor (μ') in the transformed coordinate system are related to the original ε and μ and by the relationships[6,8]

$$\varepsilon'^{i'j'} = |\det(\Lambda_i^{i'})|^{-1} \Lambda_i^{i'}\Lambda_j^{j'}, \mu'^{i'j'} = |\det(\Lambda_i^{i'})|^{-1} \Lambda_i^{i'}\Lambda_j^{i'} \mu'^{i'j'} \quad (1)$$

where $\Lambda_\alpha^{\alpha'} = \partial x'^{\alpha'}/\partial x^\alpha$ denotes the Jacobian transformation matrix between the virtual space and the original space[8].

As early as 1961, the correspondence between coordinate transformations and materials parameters had already been noted[11]. However, until about two decades ago, such correspondence was generally regarded as a mathematical technique rather than a topic for physical research. The reason is simple: from equation (1) it is clear that the transformed dielectric permittivity and magnetic permeability tensors can take on almost any local value, as the Jacobian transformation matrix is a mathematical object and, as such, is not subject to physical constraints. The close link to physics and engineering occurred with the advent of metamaterials[12,13], which not only broadened the realm of possible values for both the dielectric constant and magnetic permeability to the negative territory, but also extended their combined effect in generating negative refractive indices[14–19]. The possibility of realizing the parameter changes dictated by equation (1) may now be seriously entertained.

In 1975 it was shown that a small ellipsoid consisting of a core and a coating can have zero dipole scattering cross-section[20]. It was then reported that a negative-permittivity shell can make a positive-permittivity core invisible to external fields in the quasi-static limit[21], an effect that was subsequently found to be able to cloak discrete dipoles within a certain distance outside the shell[22]. Later, in 2005, it was shown that the scattering cross-section of a small particle can be reduced by a negative-permittivity shell[23], which is a form of approximate invisible cloaking for electromagnetic waves. In 2003, it was demonstrated that push-forward mapping[24,25] (see Box 1) can be used to design an anisotropic conductivity that renders a region undetectable by electrical impedance tomography. This is effectively an invisibility device in the quasi-static limit. In fact, the same push-forward mapping approach was later used to achieve invisibility for electromagnetic waves[2].

Two independent studies in 2006 showed that for ray optics[1] and electromagnetic waves[2] it is possible to engineer invisibility cloaks by guiding light around a region of space as if nothing is there. These reports initiated a whole series of activities that brought

[1]School of Physical Science and Technology, Soochow University, Suzhou, Jiangsu 215006, China, [2]Department of Physics and William Mong Institute of Nano Science and Technology, Hong Kong University of Science and Technology, Clear Water Bay, Hong Kong, China. *e-mail: kenyon@ust.hk

NATURE MATERIALS DOI: 10.1038/NMAT2743

Box 1 | Different types of invisibility cloaks that use materials with positive refractive index

Light propagates in a straight line in free space (**a**). By carrying out push-forward mapping to expand a point (the red dot in **a**) into a spherical hole (the red circle in **b**), light will be guided smoothly around the hole if the material inside the compressed region is prescribed according to equation (1). Outside the blue circle, the electromagnetic fields are exactly the same as in **a**, implying that any object placed inside the red circle is invisible to the observer outside the blue circle. Such push-forward mapping cloaks have extreme materials parameters (that is, they can take values of zero and infinity). Their functionality is restricted to a stationary field of single frequency. Thus for practical implementation, it is necessary to make simplifications at the expense of sacrificing some of the invisibility effect. A reduced cloak for transverse electric waves[26] was demonstrated experimentally to work at microwave frequencies by using split-ring resonators[27].

Another complementary approach is to start from geometrical optics, and use the technique of optical conformal mapping[1] to design a refractive index profile that guides rays of light around an object. Both the push-forward mapping cloak[2] and the optical conformal-mapping cloak[1] seek to use a graded medium to guide waves around a quiet region. Owing to the singularity of the coordinate transformation, the push-forward cloak can work only in a narrow bandwidth. The conformal-mapping idea, however, can use non-Euclidean geometry[52] as the starting point to get rid of extreme values of materials parameters (such as zeros or infinities) in the transformed coordinates. Thus it has the potential to achieve a broader bandwidth.

Parts **c** and **d** illustrate a mapping (in ray optics) that results in materials parameters that are less extreme. Using non-Euclidean geometry, conformal mapping can be devised so that the light rays (yellow lines) from any direction will never reach a line (or an infinitesimally thin plate, the red line in **c**), hence the line is invisible to the observer outside the blue circle. By carrying out a further transformation to expand the line (or the infinitesimally thin plate) to a closed region (the red eye in **d**), one can obtain the non-Euclidean cloak. As the transformations are non-singular, the materials parameters are less extreme.

Some strategies have been developed recently to overcome the narrow bandwidth constraint implicit in the push-forward mapping cloak. Most can be interpreted as sacrificing some degree of invisibility in return for a broader bandwidth. For example, as a line (or a thin plate) is almost invisible from at least one direction, we can do a transformation to expand the line (or a thin plate, see the red line in **e**) to a closed region (the red diamond in **f**), such that the cloaked objects have the same small cross-section as the line (or plate)[47]. The ray travelling in the same direction as the line can be cloaked (see the yellow line in **f**). Rays impinging at an angle will be reflected (see the green line in **e**). The reflected ray (green line) in **f** is exactly the same as that in **e** outside the blue box, so that observers outside the blue box will see lights as if it is reflected from a flat ground plane, and thus any object inside the red diamond is hidden. The transformation in **f** generally results in anisotropic ε and μ tensors, but using the technique of quasi-conformal mapping, the material can be reduced to an isotropic graded refractive index medium (while causing some scattering). This idea has indeed been implemented as a carpet cloak, which is broadband and has material parameters bounded in a reasonable range. There are already a few experiments[49,50,51] that have demonstrated the carpet cloak both in microwave[49] and optical frequency[50,51] regions. (Parts **a**–**d** reprinted with permission from ref. 52, © 2009 AAAS.)

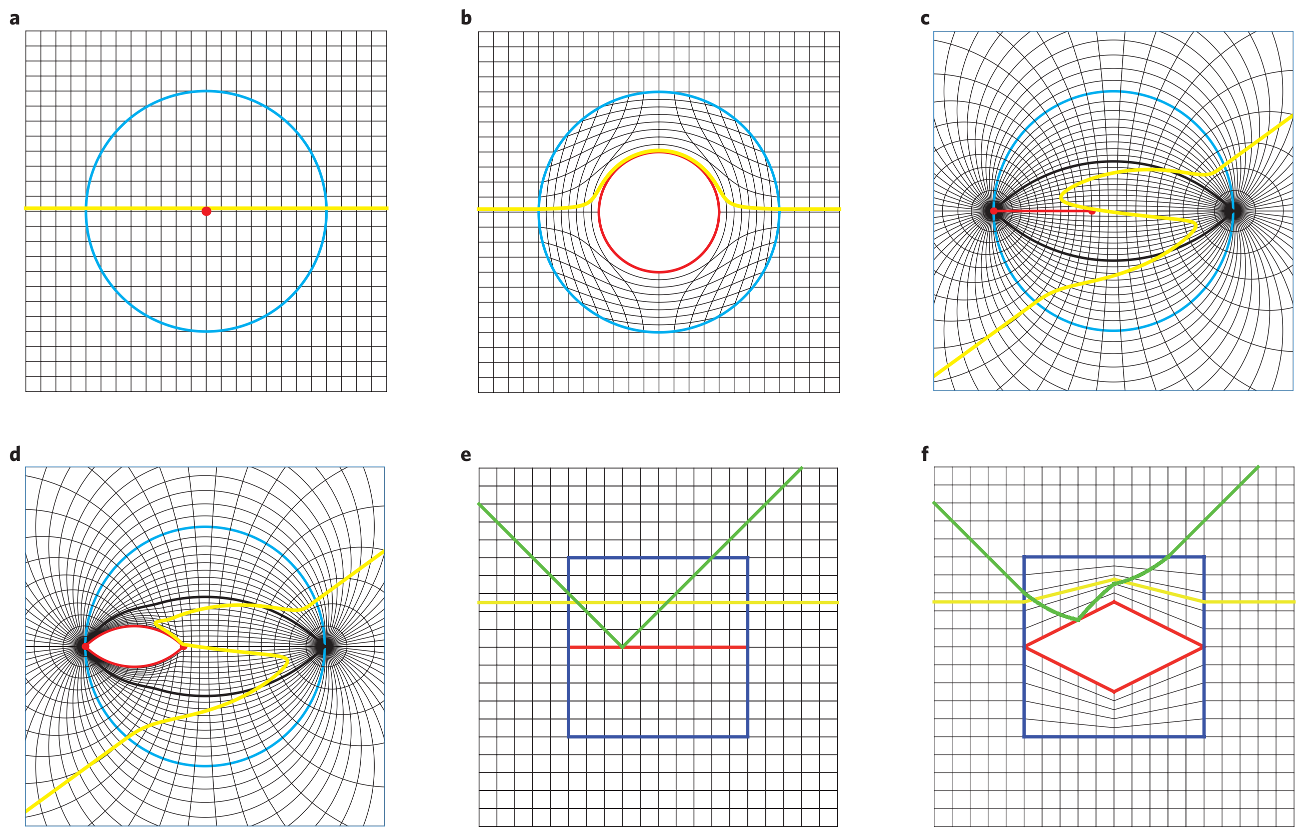

transformation optics to the attention of researchers in different disciplines around the world. The excitement was further fuelled when a 2D 'reduced' cloak[26] for transverse electric polarized waves was successfully fabricated and shown to work in the microwave frequency region[27]. Many researchers then began to look into different aspects of transformation optics. Some focused on the subtle physics of invisibility cloaks[28–33], whereas some suggested reductions (meaning simplification) for implementations in practical devices[26,34–37]. Invisibility cloaks of different forms and shapes were proposed[38–41], and designs for the operation frequency to be scaled to the optical regime for another type of polarization were also suggested[34].

One reason for the keen interest in transformation optics was the realization of something that was previously thought to be purely mathematical. The most prominent example is so-called push-forward mapping[24,25], in which a point or a line in one coordinate system is transformed to a sphere or a cylinder in another. As a point or a line is purely mathematical in character, in the sense that nothing can penetrate a point or a line — that is, they are by definition the smallest/thinnest mathematical entities — it follows that in the transformed coordinate system no wave can get into the spherical/cylindrical domain because the rule of transformation optics forces the wave to locally follow the coordinate system as it is distorted. Thus anything inside the sphere or the cylinder will become invisible[2]. This is the basis of the cloak, and the rule of the coordinate transformation directly yields the recipe for the spatial distribution of the materials parameters necessary for the realization of the cloak, in accordance with equation (1). As push-forward mapping affects only a compact region of space, it follows that the required material is also limited. In Box 1, we show an example of push-forward mapping together with its cloak region (shown as the white region in panel b). Another attractive feature of this transformation is that the required parameter values are all in the regime of positive η.

The invisibility cloak has a special mass appeal partly because it is associated with the invisibility cloak featured in the books and films of Harry Potter. Are the two really the same? From the light path in Box 1, panel b we can see that the similarity is only partially true. The fictional invisibility cloak used by Harry Potter allows him to see the outside world while his presence is concealed. Any type of cloak that works by guiding waves around a quiet region can conceal an object, but the object cannot see the outside world as no light can reach the object. One way to get around this problem is for the invisibility device not to encircle the object. This is shown to be possible by using media with negative refractive index[42,43].

The original push-forwarding mapping cloak[2] achieves perfect invisibility in one single frequency. This is inevitable because the required effective permittivity and permeability can only be realized by resonances in the building blocks of the metamaterials, and causality requirements dictate that perfect invisibility cannot have wide bandwidth[44–46]. However, the bandwidth limitation can be mitigated by sacrificing some types of functionality[44,46]. For example, the one-dimensional cloak[47] and the carpet cloak[48] can operate over a range of frequencies (the carpet cloak has been achieved both in microwave frequencies[49] and optical frequencies[50,51]); in the geometric-optics limit, a broader bandwidth cloak can be designed using non-Euclidean geometries[52]. Both are further discussed in Box. 1.

With the aid of metamaterials, the appeal of transformation optics goes beyond invisibility: it can create fascinating effects such as electromagnetic wormholes[53], hidden gateways[54,55] and 'optical black holes'[56–59]. Light-guiding and light-bending capabilities can give rise to conceptual devices such as field concentrators[60] (hyperlenses[61]), field rotators[62,63], field shifters[47,64], bending wave guides[65–70], as well as all types of lens[71–78] and advanced devices[79–82]. Eventually some may even find applications in our daily lives. As well as being a tool for designing light-bending components, transformation optics can be used to understand and interpret the intriguing optical effects of materials with negative refractive index. For example, the perfect lens[83] with $\varepsilon = \mu = -1$ can be obtained with a specific form of transformation-media mapping, called folded-geometry transformation, which makes the perfect imaging property immediately obvious[7,84]. Such a folded-geometry transformation can also lead to many interesting devices that consist of negative-index materials (NIMs). Whereas graded positive-index materials can bend light through curves in remarkable ways, NIMs can lead to unusual wave scatterings, resulting in useful effects such as the cylindrical superlens[72], scatterers with enhanced extinction cross-sections[85–87] (electromagnetic gateways[54,55]), invisible tunnels[88], focusing antennae[89,90] and optical-illusion devices[91,92].

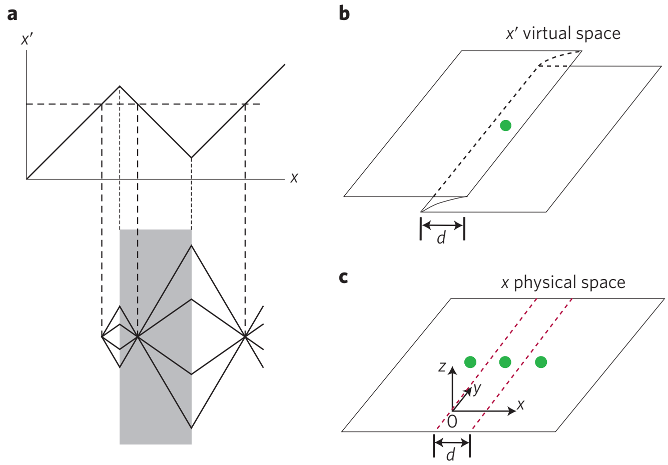

Figure 1 | The folded geometry. a, The coordinate transformation that gives the perfect lens (grey region). **b**, A point (shown in green) in the virtual space (the folded space). **c**, The point is mapped to three points in the physical space corresponding to a point source and two images, one inside the slab and one outside. Figure reprinted with permission: **a**, ref. 7, © 2006 IOP; **b**,**c**, ref. 105, © Biswajit Banerjee.

We now elaborate on a few of the effects and devices, particularly those associated with NIMs, to give a taste of the potential of transformation optics. Although most studies on transformation optics deal with electromagnetic waves, the basic principle is equally applicable to other types of wave, so long as the wave equations remain invariant under coordinate transformations. Some examples include acoustic waves[93–95], elastic waves (under certain special conditions)[96–98], matter waves[99,100], and linear (liquid) surface waves[101,102].

Materials with negative refractive index

Before the idea of transformation optics was introduced, several authors had already suggested strategies to cloak an object by cancelling wave scattering using NIMs or negative-permittivity materials. For example, a negative-permittivity shell[23] was postulated to be able to cancel the lower-order scattering of a small dielectric object. It was proved that a negative-permittivity shell (or slab) can cloak discrete dipoles within a certain distance outside the shell in the quasi-static limit[22]. However, these two methods cannot perfectly cloak an object with a size comparable to the wavelength. Here, we will review another method for perfectly cloaking an object by cancelling waves[42]. By combining the idea of transformation optics and complementary media[103], we shall see that a graded NIM can cloak an object without encircling it. Such an external cloaking action is described as cloaking at a distance[43].

A NIM is an artificial material that simultaneously possesses negative electric permittivity and negative magnetic permeability at some frequency range. A NIM has many unusual optical properties[104], but the most intriguing may be the perfect-lens effect[83]. A flat slab of a NIM with $\varepsilon = \mu = -1$ can transmit both propagating and evanescent waves perfectly in phase and in amplitude, forming a perfect image of an object placed near to it.

The astonishing lensing property of the NIM slab can be interpreted by using the idea of transformation optics. It was shown[7] that a NIM slab corresponds to a special coordinate transformation called the folded geometry[84,105]. Figure 1a shows the folded-geometry coordinate transformation from a virtual space (x') to a physical space (x). From equation (1) we can obtain the materials parameters in the physical space[7]

$$\varepsilon = \mu = \mathrm{diag}\left(\frac{\mathrm{d}x}{\mathrm{d}x'}, \frac{\mathrm{d}x'}{\mathrm{d}x}, \frac{\mathrm{d}x'}{\mathrm{d}x}\right) \tag{2}$$

where diag(...) denotes a diagonal matrix. Here, the negative slope over parts of the function (slope = –1) gives negative $\varepsilon = \mu = -1$, which is relevant for the perfect lens. Heuristically, the negative phase accumulated inside the NIM cancels exactly the positive phase in air, and hence the folded-geometry transformation is closely related to the concept of complementary media[103]. Both ideas inform us that the NIM cancels optically some of the positive-index material. We note that the solutions we shall describe for the folded geometry pertain to steady state solutions for a single frequency, and as the metamaterials required to implement folded geometry must have negative refractive index, they must be highly dispersive. We also note that when the folded geometry is used to interpret the function of a perfect lens, care should be taken in obtaining the fields in the folded region when we are considering the image of an active source[106].

Consider a point source in the folded region in the virtual space[105] (Fig. 1b). After the transformation, the virtual folded region becomes three physical regions[105] (Fig. 1c). Transformation optics (equation (2)) shows that the region in the middle[7] (grey part in Fig. 1a) actually possesses the materials parameters of a perfect lens ($\varepsilon = \mu = -1$), whereas other regions are still vacuum. The point source within a distance of $d/2$ is mapped onto two other points, one located inside the lens (Fig. 1c) and one image point outside, with a source to image distance of $2d$.

But the folded geometry actually signifies something more than what appears superficially according to the statement that some air space is cancelled (optically) by the NIM. We note that air (or a vacuum) acts like a low-pass filter, as high-spatial-frequency components exponentially decay along the propagation direction. These are the evanescent waves that hold the details of an image beyond the diffraction limit. However, if space is cancelled, there is no space for the evanescent field to decay exponentially to begin with, and thus a perfect image can be formed. This intuitive mathematical picture is supported by the fact that a NIM supports surface waves, and for the frequency at which $\varepsilon = \mu = -1$, the surface wave has a peculiar property that the surface wave dispersion has solutions for both polarizations at arbitrarily high values of the wavevector. These surface waves resonantly couple with the evanescent field to construct the perfect image. Hence the simple intuitive explanation provided by folded-geometry mapping is a valid perspective on how a perfect lens operates[7,105].

In the cylindrical or spherical geometries, the functionality of a NIM to optically cancel a positive-index medium in its vicinity has interesting implications. For example, push-forward mapping

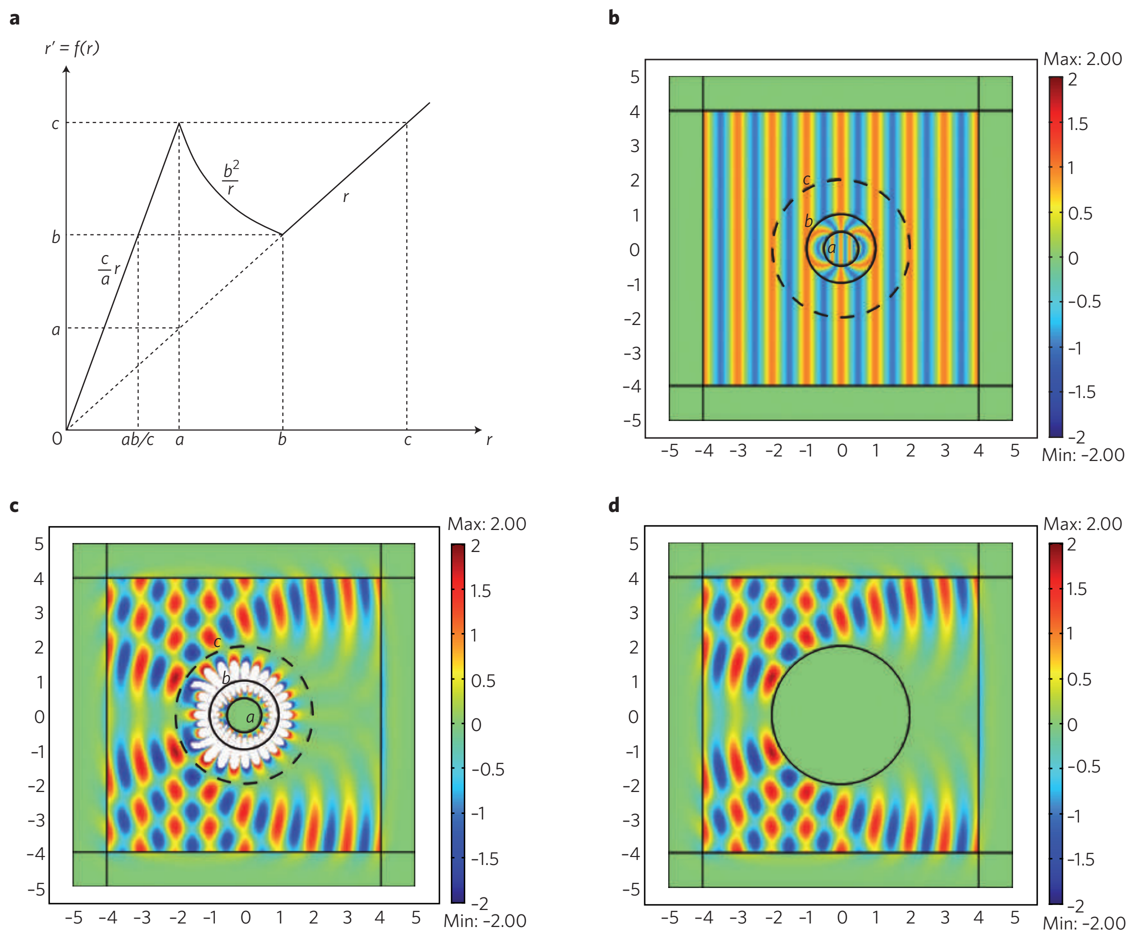

Figure 2 | The coordinate transformations that give NIMs. a, The folded-geometry transformation in the radial direction. **b**, The scattering pattern of a cylindrical perfect lens. **c**, The scattering pattern of a scatterer with enhanced scattering cross-section. **d**, The scattering pattern of a bare PEC with $a = 0.5\lambda$, $b = \lambda$ and $c = 2\lambda$. The incident waves are transverse electric polarized plane waves moving from left to right. The simulation results are calculated using the COMSOL Multiphysics finite-element-based electromagnetics solver; the coloured scale bars are in arbitrary units.

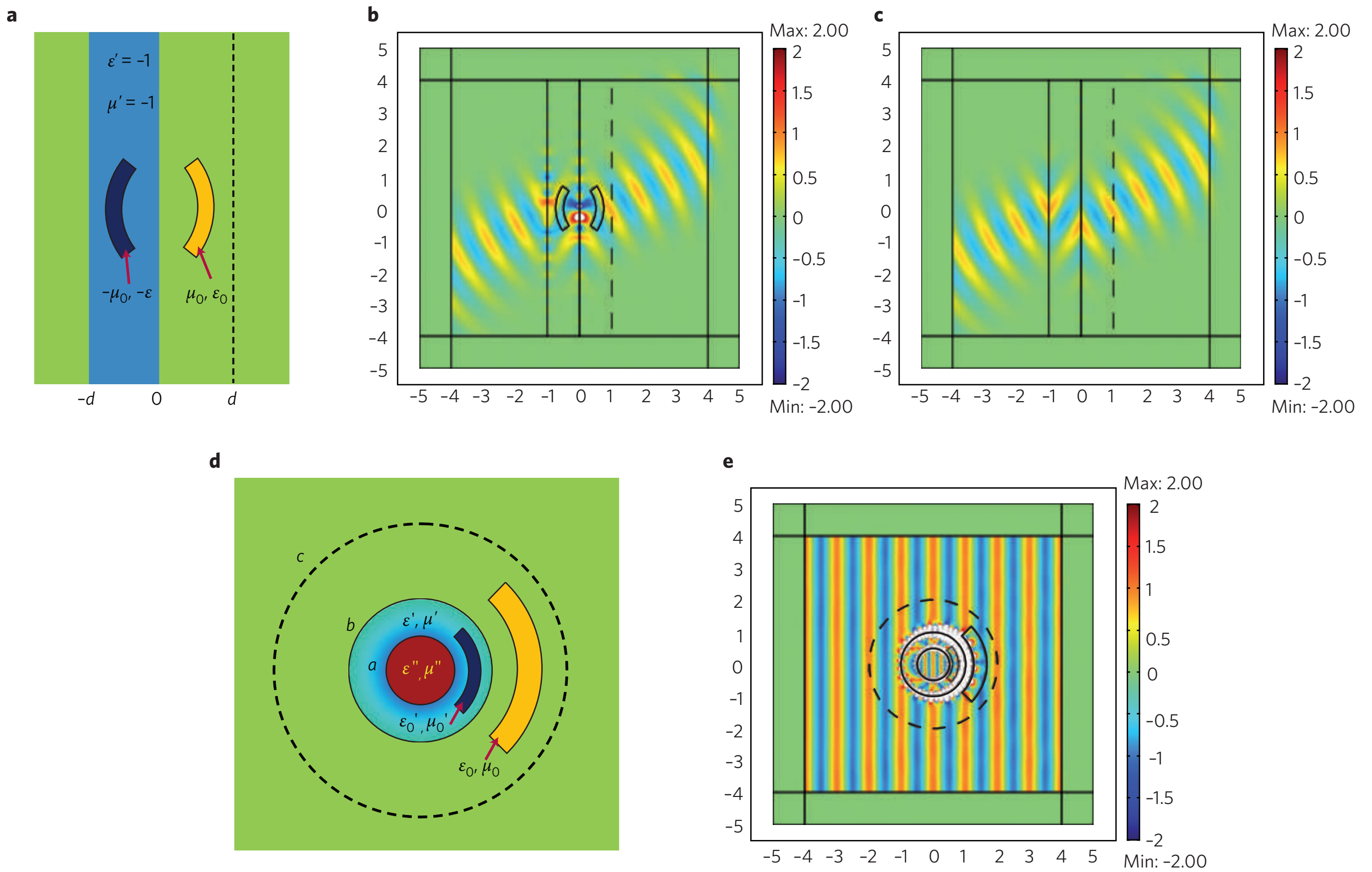

Figure 3 | Complementary media external cloak. a, A complementary media with an object (shown in yellow) in air and a NIM slab (shown in blue) with negative materials parameters $-\varepsilon(-x,y,z)$ and $-\mu(-x,y,z)$. **b**, A Gaussian beam incident at the complementary media slab depicted in **a** at a 30° angle. Here, we set $d = \lambda$. **c**, A Gaussian beam incident at the perfect lens at the same angle as in **b** but without the object and its image object counterpart. Note the similarity of the scattering pattern between panels **b** and **c**. The image object inside the NIM cancels the scattering of the object. **d**, The external cloak made by using the complementary media concept in cylindrical coordinates. **e**, The simulation results that demonstrate the external cloaking effect when the system is illuminated by a transverse electric plane wave incident from left to right. The simulation results were obtained using the COMSOL Multiphysics finite-element-based electromagnetics solver; the coloured scale bars are in arbitrary units.

should in principle cloak everything inside it[28,29]. However, an anti-cloak[107] composed of a NIM and designed using the folded-geometry transformation can partially defeat the cloaking effect of the perfect cloak that is made up of positive-index materials.

The interesting optical property of a NIM shell in the cylindrical/spherical geometry is illustrated in Fig. 2. Figure 2a shows a particular coordinate transformation from a virtual space (r') to a physical space (r) that results in a cylindrical perfect lens. The folded region in the virtual space ($b < r' < c$) is mapped onto three regions in the physical space, that is, $ab/c < r < a$, $a < r < b$ and $b < r < c$. From the transformation optics (equation (1)), the material outside the shell ($r > b$) is a vacuum. The material inside the core ($r < a$) is dielectric, and the shell itself ($a < r < b$) is a NIM. The air between ($b < r < c$) and the NIM shell between ($b < r < c$) form a pair of complementary media, and as such, the NIM shell optically cancels the air shell between $b < r < c$, so that the region bounded between $a < r < c$ is equivalent to an optical void, in which no phase is accumulated when light passes through. An optical void is not the same as a vacuum, as light can accumulate a phase change of $\int(\omega/c)\eta dx$ even if $\eta = 1$. The scattering property of the system then depends on what is placed inside the core. If the core has a material that corresponds to that at r' through a functional transformation $f(r)$, that is $r' = f(r) = (c/a)r$, then the dielectric core will compensate exactly for the missing phase in the optical-void region. For an external observer, the entire region inside $r < c$ appears optically as a region of air. From another angle, we can say that the NIM shell cancels the scattering of the dielectric core, making it perfectly transparent, or invisible. The perfect transparency under plane-wave illumination is demonstrated numerically in Fig. 2b. In contrast to the earlier work[23] that gives approximate transparency, the graded and (usually) anisotropic NIM shell corresponding to the folded-geometry transformation gives perfect transparency, that is, invisibility.

We note that in Fig. 2, the transformation $r' = f(r)$ is a continuous function from $r = 0$ to $r = c$, which ensures the impedance is matched at all values of r and thus the system is without any reflection. What if some other material is placed inside the core? We note again that the NIM serves to cancel the air shell outside it, so optically speaking, the core boundary is expanded from $r = a$ to $r = c$, and the core becomes optically equivalent to an enlarged object with diluted optical parameters. For example, if the embedded object is a perfect electric conductor (PEC), the whole device will look like another PEC with a radius c that is larger than the size of the whole device b. Hence, the effective scattering cross-section can be much larger than its geometric cross-section[21,84,85]. Figure 2c shows the scattering pattern of a PEC inside the NIM, which is the same as that of a larger PEC (see Fig. 2d). The physical basis behind such a phenomenon can be traced to the evanescent waves generated at the surfaces of the NIM shell that amplify the decaying evanescent field. This effect can be used to implement an electromagnetic gateway[54,55] that can block electromagnetic waves but allow the passage of other entities. This is another interesting

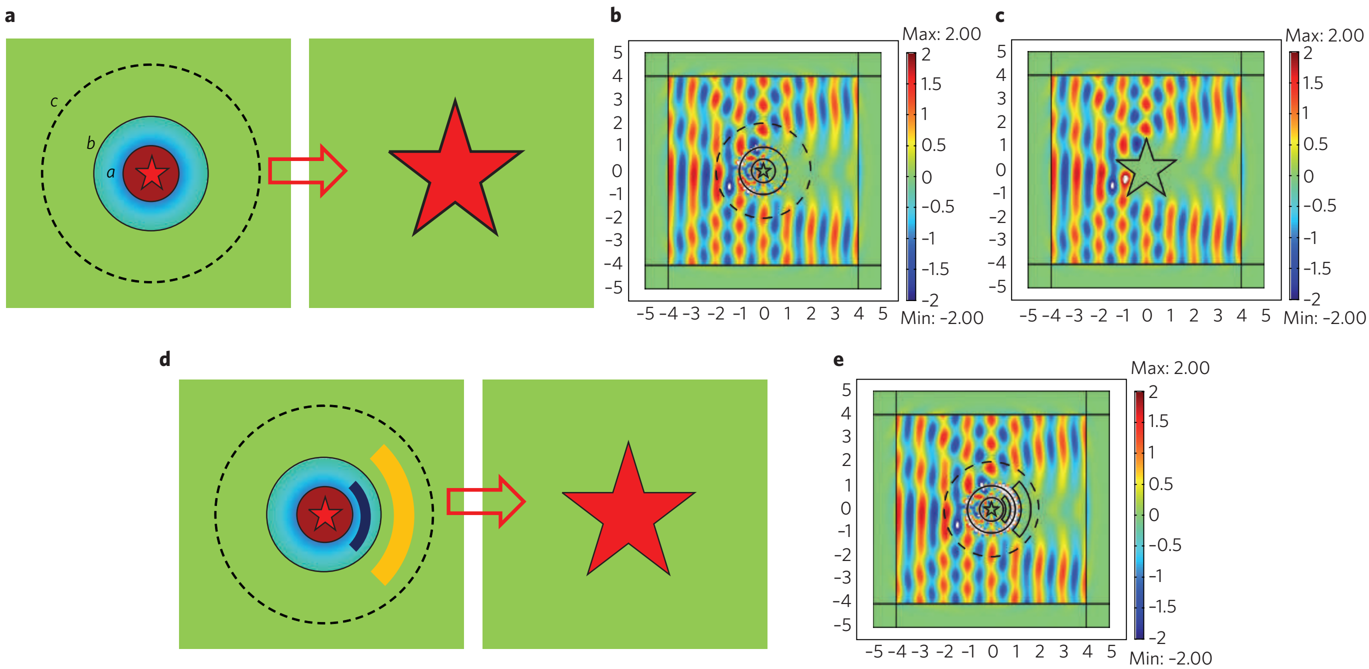

Figure 4 | Illusion optics. a, Schematic to show the projection effect of a cylindrical perfect lens. **b**, The scattering pattern of a small PEC star embedded in the dielectric core inside the NIM shell. **c**, The scattering pattern of a large PEC star in the air. Note the similarity of the scattering patterns between **b** and **c**. **d**, Schematic to illustrate the illusion effect of transforming a curved dielectric object (shown in yellow) into a star-shaped PEC object. **e**, The simulation results of the illusion effect. Note the similarity of the scattering patterns between **c** and **e**. With an incident transverse electric polarized wave propagating from left to right, the simulations were carried out using the COMSOL Multiphysics finite-element-based electromagnetics solver; the coloured scale bars are in arbitrary units. Parts **a** and **d** from ref. 92, © 2009 NPG.

example that shows that transformation optics can create unusual effects beyond merely making objects invisible.

If the embedded object is a good absorber, one can design an absorber[87] to have an effective absorbing cross-section that it is in principle much larger than its geometric cross-section and thus protect a larger area from unwanted radiation. There are some further potential applications for the folded-geometry transformation — the shifted scattering effect (which can form an image completely outside the device[86]); the invisible tunnel that can guide waves in vacuum[88]; and a focusing antenna that has a large effective diameter[89,90], to name but a few.

To summarize briefly, the perfect-lens property of a NIM slab, as explained by the complementary media concept[103], states that a NIM (where $\eta = -1$) with a layer thickness d optically cancels a slab of air ($\eta = +1$) of the same thickness, so that the information from an active source is carried forward for a distance of $2d$ without losing any information. The same is true in cylindrical and spherical geometries, and a NIM shell designed by transformation optics can serve as a cylindrical[72,108]/spherical perfect lens[86,109]. In addition to super-resolution, the NIM shell expands the $r = a$ domain (Fig. 2a) to a domain in which $r = c > a$, thereby magnifying the object.

With this in mind, we wish to show how a NIM shell designed using transformation optics can serve as a remote cloak, as well as create illusions. The concept of complementary media[103] may be generalized to a more complex configuration: a slab of inhomogeneous slab with materials parameters $\varepsilon(x,y,z)$ and $\mu(x,y,z)$ can be optically cancelled by a NIM slab with the same width and negative material parameters $-\varepsilon(-x,y,z)$ and $-\mu(-x,y,z)$, with the $x = 0$ plane being the interface[103,110]. In Fig. 3a, an object (shown in yellow) with permittivity ε_0 and permeability μ_0 is located in air near the perfect lens. The complementary media for the air layer containing the object is the $\eta = -1$ slab (shown in blue) carrying an image object (shown in dark blue) with $-\varepsilon_0$ and $-\mu_0$ (ref. 42). Fig. 3b,c shows that the image object inside the NIM slab cancels the scattering of the object in the air.

What is shown in Fig. 3a cannot be called a cloaking device, because the complementary media pair is equivalent to a region of optical void. Such a system has the drawback of being infinitely extended in the y–z plane. By applying the folded geometry in cylindrical/spherical geometries using the transformation introduced in Fig. 2a, a true cloak can be created. Consider the configuration depicted in Fig. 3d. The air region between ($b < r < c$) and the NIM between ($a < r < b$) form a pair of complementary media. The configuration shown in Fig. 3d can be regarded as the generalization of the perfectly transparent configuration shown in Fig. 2b, except that the positive-index shell now carries an object (shown in yellow) and the NIM has to carry an image object. We note that the dielectric core is needed to compensate for the missing phase in the optical-void area between $a < r < c$. From the point of view of an external observer, an object with ε_0 and μ_0 in the range $b < r < c$ (see Fig. 3d) is cloaked by the device bounded by $r < b$, which contains a dielectric core and a NIM cylindrical perfect lens carrying an embedded image with opposite materials parameters. The image object is called the anti-object, for which the shape and materials parameters can be calculated from the transformation optics[42]. The NIM shell with an embedded anti-object can cloak an object without touching or enclosing it, hence the use of the terms external cloak or cloaking at a distance[43]. The cloaking effect is demonstrated in Fig. 3e for a plane wave incident from the left. We note that such complementary-media-based invisibility devices work for any type of external light sources and do not have to be cylindrical or spherical. Similar concepts may be applied to other shapes of perfect lenses[55,111].

Although a NIM can function as a complementary medium[42,103] to cancel the scatterings, it can also function as a lens[103] to project an image. Figure 4a shows an illustration of the cylindrical NIM lens projecting a star-shaped PEC, located inside the dielectric core, into a real image in air with a larger size. An observer outside the dashed circle will see a bigger star-shaped object rather than the original one embedded in the dielectric core. Figure 4b demonstrates such an effect by full wave simulation, which shows that the scattering pattern of a star-shaped object embedded inside the NIM shell is the same as the scattering pattern of a larger star in air (Fig. 4c). By combining the two functionalities, and using transformation-media methodology, a conceptual device can be visualized that optically transforms one object into another[91] (for example, a curved dielectric object (shown in yellow) appears as a star to a far-field observer, as shown schematically in Fig. 4d). The curved dielectric object is cloaked by embedding an anti-object in the cylindrical perfect lens. A small star-shaped object inside the dielectric core is then projected into a larger star so that the curved dielectric object actually looks like a star for the far-field observer. Figure 4e shows the simulation results demonstrating the illusion effect. When the conceptual device is placed near a curved dielectric object, the scattering pattern is essentially the same as that of a star. An observer outside $r = c$ (the dashed circle) will see nothing but a star. We note that the functionality of the illusion device is independent of the nature of the external light source as long as the sources are outside the boundary, that is, where $r = c$. Such an effect raises an interesting philosophical issue: can you believe what you see if the information is obtained at only one frequency?

Besides the simple example above, there are other applications, for example an illusion device that would allow people to see through walls[91]. It should be noted that the folded-geometry transformations that lead to different types of perfect lens[55,111] can also have their corresponding illusion devices.

Implementing the illusion-optics devices presents several challenges: the key component of illusion optics is a NIM shell. As a NIM needs resonance to achieve negative materials parameters, it will have inevitable bandwidth limitations. In addition, the cloaking or illusion effect has to be tailor-made for the object to be cloaked, as an anti-object is needed to carry out the wave-scattering cancellation. Owing to the rapid advances in metamaterial fabrication technology[49], it might be possible to obtain some proof-of-concept demonstrations on illusion devices in the microwave regime. However, it would be a real challenge to implement a device in the optical frequency region, owing to both material losses and the difficulties in fabrication[19].

New wave-manipulation strategies

There are of course many other forms of coordinate transformation that take us beyond making objects invisible. For example, the radial mapping shown in Fig. 5a can produce a field concentrator[60]. Figure 5b shows a field concentrator that can concentrate the energy in a small region $r < a$ while the device itself is invisible as the system does not cause any scattering (for details, see ref. 60).

Although push-forward-type mapping has focused on coordinate transformations along the radial direction of the cylindrical/spherical coordinates, angular transformation would also lead to interesting effects. For example, angular mapping can result in a field rotator (see Fig. 5c) that rotates the fields so that the information from inside ($r < a$) or outside ($r > b$) a shell will appear as if it comes from a different angle[62]. The mapping is performed for the region $r < b$. Inside the region $r = a$, the whole domain is transformed by rotating a fixed angle (here, for example, 90°) from the region $r' = a$ in virtual space, and for the region between $a < r < b$, the rotation angle is continually changed from the fixed angle to zero. By putting a scatterer inside the rotator (Fig. 5d), the far-field observer will see a rotated image (Fig. 5e); the same scattering pattern outside $r = b$ is shown

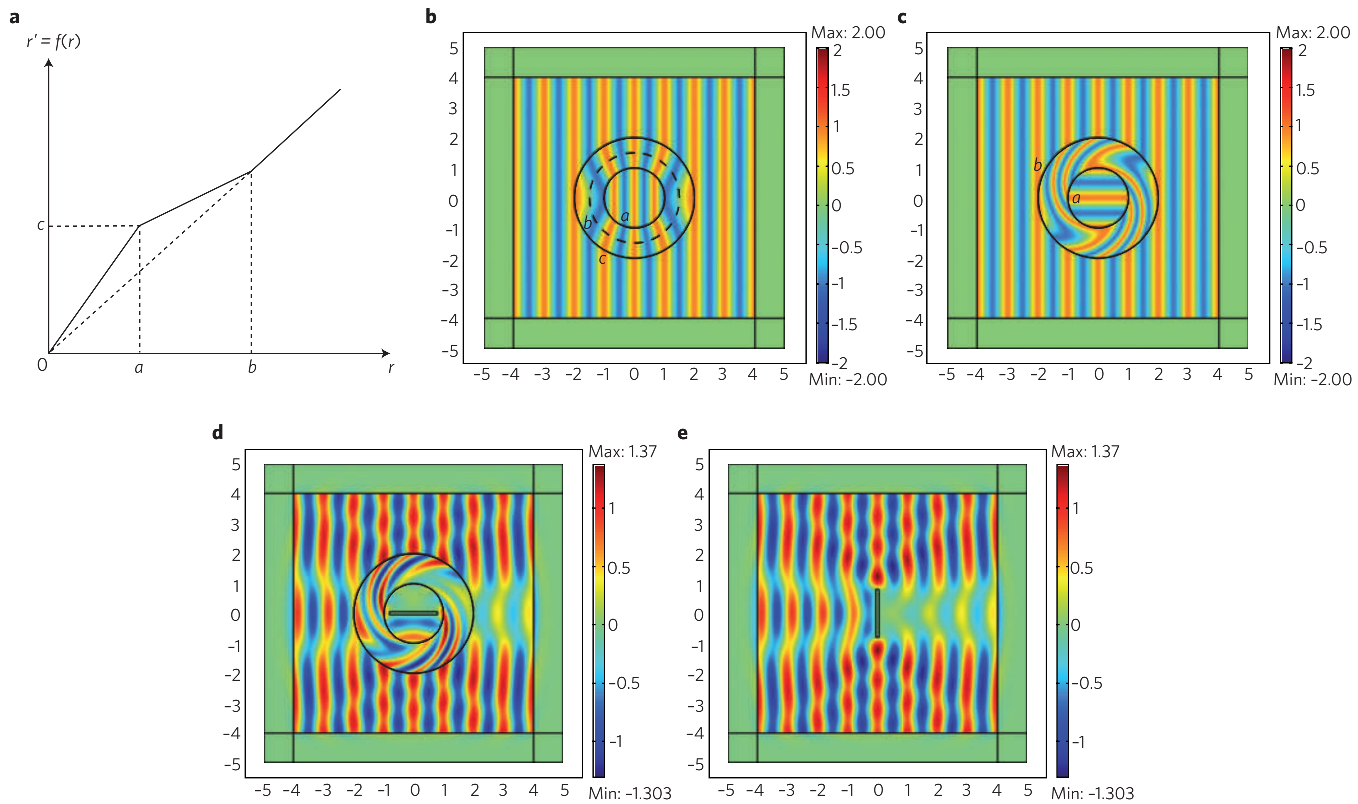

Figure 5 | A field concentrator and a field rotator. a, The coordinate transformation that gives an invisible field concentrator. The transformation function is $r' = f(r) = (c/a)r$ for $0 < r < a$; $((b - c)/(b - a))(r - b) + b$ for $a < r < b$; and r for $r > b$. **b**, The scattering pattern of the invisible field concentrator. **c**, The scattering pattern of an invisible field rotator that rotates wave fronts by 90°. **d**, The scattering pattern for a plate lying on the x axis inside the rotator. **e**, The scattering pattern of a plate lying on the y axis in air. Note the similarity of the scattering patterns in **d** and **e**. Here we set $a = \lambda$, $b = 2\lambda$ and $c = 1.5\lambda$. The incident wave is a transverse magnetic polarized plane wave moving from left to right. The simulation results are calculated from the COMSOL Multiphysics finite-element-based electromagnetics solver; the coloured scale bars are in arbitrary units.

in Fig. 5d,e. We can see from Fig. 5c that the field rotator itself is invisible, so that it can be regarded as another type of optical-illusion device that leads the observer to think that information is actually coming from an imaginary direction. The field rotator can be implemented by using alternating fan-shaped layered systems with only two kinds of isotropic materials[47]; a proof-of-principle demonstration was realized using a very simple structure consisting of an array of identical aluminium metal plates[63].

Transformation optics has now been used as a versatile tool in designing many potential applications. Here we give an incomplete list. An impedance-matched hyperlens[61] was proposed to reduce the scattering on the surfaces of the hyperlens based on the same mapping as the field concentrator. A transmuted Eaton lens[77] was demonstrated in a microwave experiment[78] to realize a cat's eye for all directions[112]. Also proposed were transformation media waveguides[65–69] that can guide waves smoothly around the bending part of a waveguide by mapping a rectangular region in virtual space into a bending physical space, a process based on the principles of embedded transformation optics. Such a bending transformation media waveguide was recently achieved in a microwave experiment[70]. A wave shifter\splitter\combiner[47,64] was suggested as a means to shift, split and combine waves based on a simple shift mapping that can be implemented by using an alternating layered system with several types of isotropic material. Optical guiding can also be achieved by graded refractive index media designed with approximate forms of transformation optics[48]. In particular, if techniques such as quasi-conformal mapping are used, the graded refractive index material can be implemented with pure dielectrics, resulting in low loss and broadband functionality. Such devices can have plausible on-chip optics applications. There are also many transformation media designs as discussed in the introduction, both for possible applications and for new effects that challenge our imagination. We cannot possibly give a comprehensive review of this topic simply because it is advancing so rapidly. By introducing the basic elements of transformation optics and some of its applications in conjunction with NIMs, we hope to make apparent not only the simple and beautiful mathematical construct of the approach, but also the materials-based underpinnings that are required for realizing its full potential.

Concluding remarks

Transformation optics offers a way to control light with a seemingly mysterious quality. The invisibility cloak is one of the most exciting examples. Some of the ideas have already been demonstrated in proof-of-principle experiments carried out across several frequencies ranging from the microwave[27,49,113] to the optical regions[50,51,114].

Although most invisibility cloaks are based on graded positive-index materials, NIMs can also be used to create the invisibility effect. In general, a graded positive-index shell can conceal an enclosed object by steering light around it, whereas a NIM shell can render an external object invisible by scattering cancellation. The parameters of NIMs can be obtained with folded-geometry transformations, which can also be used to create many illusion effects, such as scatterers that appear much larger than their geometric cross-sections. An intriguing extension of the ideas is to use NIMs to design illusion devices such that one object can be optically transformed into another.

We have focused on transformation media that use passive materials. Similar effects can also be achieved by using active sources that either enclose[115] or encircle the cloaked region[116]. An advantage of active-source cloaking is that it does not have the difficulties in fabrication that are inherent to metamaterials, as well as the associated bandwidth limitations, but it requires the knowledge of incoming waves, which in itself is a challenge for high-frequency applications. Other cloaking techniques have also been proposed[117], which attempt to reduce total scattering cross-sections of objects by using metals with elongated shapes and hard surfaces[118] or by using volumetric transmission-line techniques[119].

It is possible to foresee a proliferation in the use of transformation optics as a design tool, and the two aspects — nano-/microstructured composites and target-oriented designed — will serve as a synergistic driver for the realization of new wave-manipulation devices. In particular, it is possible to predict some of the optical effects created by transformation optics being integrated into photonic chips to broaden their functionalities, or offering alternative routes to high-resolution imaging. All of the aforementioned discussion on transformation optics assumes a linear response of the metamaterial to the external field. It would be a challenge for theory to treat nonlinear effects, but it may be a worthwhile future step as nonlinear or tunable metamaterials[120–129] can be very useful for some applications. In the short-term, more experimental work to demonstrate the feasibility of transformation-optics-based devices would be highly desirable. Proof-of-concept experiments carried out at microwave frequencies should be feasible. The ultimate goal would be to realize useful devices at higher frequencies, or even at optical frequencies, but this objective will probably be hampered by several difficulties. The most challenging issue is perhaps the issue of materials loss at optical frequencies, which is particularly serious when nanoplasmonic structures are used. It was shown that surface roughness and quantum size effects play important roles for losses at the plasmon resonances[130]. To overcome the loss, the search for new plasmonic materials[131–133] and/or the use of gain to compensate for loss[134–136] have been proposed. The bandwidth limitation is another key challenge that must be overcome. As perfect functionalities (such as perfect cloaking) and large operating bandwidth are mutually exclusive, there is a need to strike an optimal balance between the two for any particular application.

References

1. Leonhardt, U. Optical conformal mapping. *Science* **312,** 1777–1780 (2006).
2. Pendry, J. B., Schurig, D. & Smith, D. R. Controlling electromagnetic fields. *Science* **312,** 1780–1782 (2006).
3. Ramo, S., Whinnery, J. R. & Van Duzer, T. *Fields and Waves in Communication Electronics* 3rd edn, Ch. 7 (Wiley, 1994).
4. Post, E. G. *Formal Structure of Electromagnetics: General Covariance and Electromagnetics* (Interscience Publishers, 1962).
5. Lax, M. & Nelson, D. F. Maxwell equations in material form. *Phys. Rev. B* **13,** 1777–1784 (1976).
6. Schurig, D., Pendry, J. B. & Smith, D. R. Calculation of material properties and ray tracing in transformation media. *Opt. Express* **14,** 9794–9804 (2006).
7. Leonhardt, U. & Philbin, T. G. General relativity in electrical engineering. *New J. Phys.* **8,** 247 (2006).
8. Milton, G. W., Briane, M. & Willis, J. R. On cloaking for elasticity and physical equations with a transformation invariant form. *New J. Phys.* **8,** 248 (2006).
9. Shalaev, V. M. Transforming light. *Science* **322,** 384–386 (2008).
10. Leonhardt, U. & Philbin, T. G. Transformation optics and the geometry of light. *Prog. Opt.* **53,** 69–152 (2009).
11. Dolin, L. S. On a possibility of comparing three-dimensional electromagnetic systems with inhomogeneous filling. *Izv. Vuz. Radiofiz.* **4,** 964–967 (1961).
12. Pendry, J. B. *et al.* Extremely low frequency plasmons in metallic mesostructures. *Phys. Rev. Lett.* **76,** 4773–4776 (1996).
13. Pendry, J. B. *et al.* Magnetism from conductors and enhanced nonlinear phenomena. *IEEE Trans. Microwave Theory* **47,** 2075–2084 (1999).
14. Shelby, R. A., Smith, D. R. & Schultz, S. Experimental verification of a negative index of refraction. *Science* **292,** 77–79 (2001).
15. Smith, D. R., Pendry, J. B. & Wiltshire, M. C. K. Metamaterials and negative refractive index. *Science* **305,** 788–792 (2004).
16. Soukoulis, C. M., Linden, S. & Wegener, M. Negative refractive index at optical wavelengths. *Science* **315,** 47–49 (2007).
17. Lezec, H. J., Dionne, J. A. & Atwater, H. A. Negative refraction at visible frequencies. *Science* **316,** 430–432 (2007).
18. Yao, J. *et al.* Optical negative refraction in bulk metamaterials of nanowires. *Science* **321,** 930 (2008).
19. Valentine, J. *et al.* Three-dimensional optical metamaterial with a negative refractive index. *Nature* **455,** 376–379 (2008).
20. Kerker, M. Invisible bodies. *J. Opt. Soc. Am.* **65,** 376–379 (1975).
21. Nicorovici, N. A., McPhedran, R. C. & Milton, G. W. Optical and dielectric properties of partially resonant composites. *Phys. Rev. B* **49,** 8479–8482 (1994).

22. Milton, G. W. & Nicorovici, N-A. P. On the cloaking effects associated with anomalous localized resonance. *Proc. R. Soc. Lon. Ser.-A* **462,** 3027–3059 (2006).
23. Alù, A. & Engheta, N. Achieving transparency with plasmonic and metamaterial coatings. *Phys. Rev. E* **72,** 016623 (2005).
24. Greenleaf, A., Lassas, M. & Uhlmann, G. On non-uniqueness for Calderon's inverse problem. *Math. Res. Lett.* **10,** 685–693 (2003).
25. Greenleaf, A., Lassas, M. & Uhlmann, G. Anisotropic conductivities that cannot be detected by EIT. *Physiol. Meas*. **24,** 413–419 (2003).
26. Cummer, S. A. *et al.* Full-wave simulations of electromagnetic cloaking structures. *Phys. Rev. E* **74,** 036621 (2006).
27. Schurig, D. *et al.* Metamaterial electromagnetic cloak at microwave frequencies. *Science* **314,** 977–980 (2006).
28. Chen, H. S. *et al.* Electromagnetic wave interactions with a metamaterial cloak. *Phys. Rev. Lett.* **99,** 063903 (2007).
29. Ruan, Z. C. *et al.* Ideal cylindrical cloak: perfect but sensitive to tiny perturbations. *Phys. Rev. Lett.* **99,** 113903 (2007).
30. Yan, M., Ruan, Z. & Qiu, M. Cylindrical invisibility cloak with simplified material parameters is inherently visible. *Phys. Rev. Lett.* **99,** 233901 (2007).
31. Liang, Z. X. *et al.* The physical picture and the essential elements of the dynamical process for dispersive cloaking structures. *Appl. Phys. Lett.* **92,** 131118 (2008).
32. Chen, H. Y. & Chan, C. T. Time delays and energy transport velocities in three dimensional ideal cloaking devices. *J. Appl. Phys.* **104,** 033113 (2008).
33. Leonhardt, U. Notes on conformal invisibility devices. *New J. Phys.* **8,** 118 (2006).
34. Cai, W. S. *et al.* Optical cloaking with metamaterials. *Nature Photon.* **1,** 224–227 (2007).
35. Cai, W. S. *et al.* Nonmagnetic cloak with minimized scattering. *Appl. Phys. Lett.* **91,** 111105 (2007).
36. Wood, B. & Pendry, J. B. Metamaterials at zero frequency. *J. Phys. Condens. Matter* **19,** 076208 (2007).
37. Magnus, F. *et al.* A d.c. magnetic metamaterial. *Nature Mater.* **7,** 295–297 (2008).
38. Yan, W. *et al.* Coordinate transformations make perfect invisibility cloaks with arbitrary shape. *New J. Phys.* **10,** 043040 (2008).
39. Jiang, W. X. *et al.* Arbitrarily elliptical–cylindrical invisible cloaking. *J. Phys. D* **41,** 085504 (2008).
40. Kwon, D.-H. & Werner, D. H. Two-dimensional eccentric elliptic electromagnetic cloaks. *Appl. Phys. Lett.* **92,** 013505 (2008).
41. Nicolet, A., Zolla, F. & Guenneau, S. Electromagnetic analysis of cylindrical cloaks of an arbitrary cross section. *Opt. Lett.* **33,** 1584–1586 (2008).
42. Lai, Y. *et al.* Complementary media invisibility cloak that cloaks objects at a distance outside the cloaking shell. *Phys. Rev. Lett.* **102,** 093901 (2009).
43. Philbin, T. Cloaking at a distance. *Physics* **2,** 17 (2009).
44. Chen, H. Y. *et al.* Extending the bandwidth of electromagnetic cloaks. *Phys. Rev. B* **76,** 241104 (2007).
45. Yaghjian, A. D. & Maci, S. Alternative derivation of electromagnetic cloaks and concentrators. *New J. Phys.* **10,** 115022 (2008).
46. Kildishev, A. V. *et al.* Transformation optics: Approaching broadband electromagnetic cloaking. *New J. Phys.* **10,** 115029 (2008).
47. Chen, H. Y. & Chan, C. T. Electromagnetic wave manipulation by layered systems using the transformation media concept. *Phys. Rev. B* **78,** 054204 (2008).
48. Li, J. & Pendry, J. B. Hiding under the carpet: A new strategy for cloaking. *Phys. Rev. Lett.* **101,** 203901 (2008).
49. Liu, R. *et al.* Broadband ground-plane cloak. *Science* **323,** 366–369 (2009).
50. Valentine, J. *et al.* An optical cloak made of dielectrics. *Nature Mater.* **8,** 568–571 (2009).
51. Gabrielli, L. H. *et al.* Silicon nanostructure cloak operating at optical frequencies. *Nature Photon.* **3,** 461–463 (2009).
52. Leonhardt, U. & Tyc, T. Broadband invisibility by non-Euclidean cloaking. *Science* **323,** 110–112 (2009).
53. Greenleaf, A., Lassas, M. & Uhlmann, G. Electromagnetic wormholes and virtual magnetic monopoles from metamaterials. *Phys. Rev. Lett.* **99,** 183901 (2007).
54. Luo, X. D. *et al.* Conceal an entrance by means of superscatterer. *Appl. Phys. Lett.* **94,** 223513 (2009).
55. Chen, H. Y. *et al.* A simple route to a tunable electromagnetic gateway. *New J. Phys.* **11,** 083012 (2009).
56. Leonhardt, U. & Piwnicki, P. Optics of nonuniformly moving media. *Phys. Rev. A* **60,** 4301–4312 (1999).
57. Genov, D. A., Zhang, S. & Zhang, X. Mimicking celestial mechanics in metamaterials. *Nature Phys.* **5,** 687–692 (2009).
58. Narimanov, E. E. & Kildishev, A. V. Optical black hole: Broadband omnidirectional light absorber. *Appl. Phys. Lett.* **95,** 041106 (2009).
59. Cheng, Q. & Cui, T. J. An electromagnetic black hole made of metamaterials. Preprint at <http://arxiv.org/abs/0910.2159> (2009).
60. Rahm, M. *et al.* Design of electromagnetic cloaks and concentrators using form-invariant coordinate transformations of Maxwells equations. *Photon. Nanostr.* **6,** 87–95 (2008).
61. Kildishev, A. V. & Narimanov, E. E. Impedance-matched hyperlens. *Opt. Lett.* **32,** 3432–3434 (2007).
62. Chen, H. Y. & Chan, C. T. Transformation media that rotate electromagnetic fields. *Appl. Phys. Lett.* **90,** 241105 (2007).
63. Chen, H. Y. *et al.* Design and experimental realization of a broadband transformation media field rotator at microwave frequencies. *Phys. Rev. Lett.* **102,** 183903 (2009).
64. Rahm, M. *et al.* Optical design of reflectionless complex media by finite embedded coordinate transformations. *Phys. Rev. Lett.* **100,** 063903 (2008).
65. Huangfu, J. T. *et al.* Application of coordinate transformation in bent waveguides. *J. Appl. Phys.* **104,** 014502 (2008).
66. Roberts, D. A. *et al.* Transformation-optical design of sharp waveguide bends and corners. *Appl. Phys. Lett.* **93,** 251111 (2008).
67. Rahm, M. *et al.* Transformation-optical design of adaptive beam bends and beam expanders. *Opt. Express* **16,** 11555–11567 (2008).
68. Jiang, W. X. *et al.* Arbitrary bending of electromagnetic waves using realizable inhomogeneous and anisotropic materials. *Phys. Rev. E* **78,** 066607 (2008).
69. Mei, Z. L. & Cui, T. J. Arbitrary bending of electromagnetic waves using isotropic materials. *J. Appl. Phys.* **105,** 104913 (2009).
70. Mei, Z. L. & Cui, T. J. Experimental realization of a broadband bend structure using gradient index metamaterials. *Opt. Express* **17,** 18354–18363 (2009).
71. Tsang, M. & Psaltis, D. Magnifying perfect lens and superlens design by coordinate transformation. *Phys. Rev. B* **77,** 035122 (2008).
72. Yan, M., Yan, W. & Qiu, M. Cylindrical superlens by a coordinate transformation. *Phys. Rev. B* **78,** 125113 (2008).
73. Jiang, W. X. *et al.* Layered high-gain lens antennas via discrete optical transformation. *Appl. Phys. Lett.* **93,** 221906 (2008).
74. Kwon, D-H. & Werner, D. H. Flat focusing lens designs having minimized reflection based on coordinate transformation techniques. *Opt. Express* **17,** 7807–7817 (2009).
75. Roberts, D. A., Kundtz, N. & Smith, D. R. Optical lens compression via transformation optics. *Opt. Express* **17,** 16535–16542 (2009).
76. Li, J. *et al.* Designing the Fourier space with transformation optics. *Opt. Lett.* **34,** 3128–3130 (2009).
77. Tyc, T. & Leonhardt, U. Transmutation of singularities in optical instruments. *New J. Phys.* **10,** 115038 (2008).
78. Ma, Y. G. *et al.* An omnidirectional retroreflector based on the transmutation of dielectric singularities. *Nature Mater.* **8,** 639–642 (2009).
79. Kwon, D-H. & Werner, D. H. Polarization splitter and polarization rotator designs based on transformation optics. *Opt. Express* **16,** 18731–18738 (2008).
80. Jiang, W. X. *et al.* Cylindrical-to-plane-wave conversion via embedded optical transformation. *Appl. Phys. Lett.* **92,** 261903 (2008).
81. Ma, H. *et al.* Wave-shape-keeping media. *Opt. Lett.* **34,** 127–129 (2009).
82. Zhai, T. R. *et al.* Polarization controller based on embedded optical transformation. *Opt. Express* **17,** 17206–17213 (2009).
83. Pendry, J. B. Negative refraction makes a perfect lens. *Phys. Rev. Lett.* **85,** 3966–3969 (2000).
84. Milton, G. W. *et al.* Solutions in folded geometries, and associated cloaking due to anomalous resonance. *New J. Phys.* **10,** 115021 (2008).
85. Yang, T. *et al.* Superscatterer: Enhancement of scattering with complementary media. *Opt. Express* **16,** 18545–18550 (2008).
86. Luo, Y. *et al.* Wave and ray analysis of a type of cloak exhibiting magnified and shifted scattering effect. *Pr. Electromag. Res. S.* **95,** 167–178 (2009).
87. Ng, J., Chen, H. Y. & Chan, C. T. Metamaterial frequency-selective superabsorber. *Opt. Lett.* **34,** 644–646 (2009).
88. Zhang, J. J. *et al.* Guiding waves through an invisible tunnel. *Opt. Express* **17,** 6203–6208 (2009).
89. Lu, W. L. *et al.* Transformation media based super focusing antenna. *J. Phys. D* **42,** 212002 (2009).
90. Luo, Y. *et al.* High-directivity antenna with small antenna aperture. *Appl. Phys. Lett.* **95,** 193506 (2009).
91. Lai, Y. *et al.* Illusion optics: The optical transformation of an object into another object. *Phys. Rev. Lett.* **102,** 253902 (2009).
92. Pendry, J. B. Optics: All smoke and metamaterials. *Nature* **460,** 579–580 (2009).
93. Cummer, S. A. & Schurig, D. One path to acoustic cloaking. *New J. Phys.* **9,** 45 (2007).
94. Chen, H. Y. & Chan, C. T. Acoustic cloaking in three dimensions using acoustic metamaterials. *Appl. Phys. Lett.* **91,** 183518 (2007).
95. Cummer, S. A. *et al.* Scattering theory derivation of a 3D acoustic cloaking shell. *Phys. Rev. Lett.* **100,** 024301 (2008).
96. Brun, M., Guenneau, S. & Movchan, A. B. Achieving control of in-plane elastic waves. *Appl. Phys. Lett.* **94,** 061903 (2009).
97. Farhat, M. *et al.* Cloaking bending waves propagating in thin elastic plates. *Phys. Rev. B* **79,** 033102 (2009).

NATURE MATERIALS DOI: 10.1038/NMAT2743

98. Farhat, M., Guenneau, S. & Enoch, S. Ultrabroadband elastic cloaking in thin plates. *Phys. Rev. Lett.* **103,** 024301 (2009).
99. Zhang, S. *et al.* Cloaking of matter waves. *Phys. Rev. Lett.* **100,** 123002 (2008).
100. Lin, D-H. & Luan, P-G. Cloaking of matter waves under the global Aharonov–Bohm effect. *Phys. Rev. A* **79,** 051605 (2009).
101. Farhat, M. *et al.* Broadband cylindrical acoustic cloak for linear surface waves in a fluid. *Phys. Rev. Lett.* **101,** 134501 (2008).
102. Chen, H. Y. *et al.* Transformation media for linear liquid surface waves. *Europhys. Lett.* **85,** 24004 (2009).
103. Pendry, J. B. & Ramakrishna, S. A. Focusing light using negative refraction. *J. Phys. Condens. Matter* **15,** 6345–6364 (2003).
104. Veselago, V. G. The electrodynamics of substances with simultaneously negative values of ε and μ. *Sov. Phys. Uspekhi* **10,** 509–514 (1968).
105. Milton, G. W. Fig. 2 in http://en.wikiversity.org/wiki/Waves_in_composites_and_metamaterials/Transformation-based_cloaking_in_mechanics (2009).
106. Bergamin, L. & Favara, A. Negative index of refraction, perfect lenses and transformation optics — some words of caution. Preprint at <http://arxiv.org/abs/1001.4655> (2010).
107. Chen, H. Y. *et al.* The anti-cloak. *Opt. Express* **16,** 14603–14608 (2008).
108. Pendry, J. B. Perfect cylindrical lenses. *Opt. Express* **11,** 755–760 (2003).
109. Rmakrishna, S. A. & Pendry, J. B. Spherical perfect lens: solutions of Maxwell's equations for spherical geometry. *Phys. Rev. B* **69,** 115115 (2004).
110. Zheng, G., Heng, X. & Yang, C. A phase conjugate mirror inspired approach for building cloaking structures with left-handed materials. *New J. Phys.* **11,** 033010 (2009).
111. Chen, H. Y. & Chan, C. T. "Cloaking at a distance" from folded geometries in bipolar coordinates. *Opt. Lett.* **34,** 2649–2651 (2009).
112. Dennis, M. R. A cat's eye for all directions. *Nature Mater.* **8,** 613–614 (2009).
113. Tretyakov, S. *et al.* Broadband electromagnetic cloaking of long cylindrical objects. *Phys. Rev. Lett.* **103,** 103905 (2009).
114. Smolyaninov, I. I. *et al.* Anisotropic metamaterials emulated by tapered waveguides: Application to optical cloaking. *Phys. Rev. Lett.* **102,** 213901 (2009).
115. Miller, D. A. B. On perfect cloaking. *Opt. Express* **14,** 12457–12466 (2006).
116. Vasquez, F. G., Milton, G. W. & Onofrei, D. Active exterior cloaking for the 2D Laplace and Helmholtz equations. *Phys. Rev. Lett.* **103,** 073901 (2009).
117. Alitalo, P. & Tretyakov, S. Electromagnetic cloaking with metamaterials. *Mater. Today* **12,** 22–29 (2009).
118. Kildal, P-S., Kishk, A. A. & Tengs, A. Reduction of forward scattering from cylindrical objects using hard surfaces. *IEEE T. Antenn. Propag.* **44,** 1509–1520 (1996).
119. Alitalo, P. *et al.* Transmission-line networks cloaking objects from electromagnetic fields. *IEEE T. Antenn. Propag.* **56,** 416–424 (2008).
120. Zharov, A. A., Shadrivov, I. V. & Kivshar, Y. S. Nonlinear properties of left-handed metamaterials. *Phys. Rev. Lett.* **91,** 037401 (2003).
121. Agranovich, V. M. *et al.* Linear and nonlinear wave propagation in negative refraction metamaterials. *Phys. Rev. B* **69,** 165112 (2004).
122. O'Brien, S. *et al.* Near-infrared photonic band gaps and nonlinear effects in negative magnetic metamaterials. *Phys. Rev. B* **69,** 241101(R) (2004).
123. Liu, Y. *et al.* Subwavelength discrete solitons in nonlinear metamaterials. *Phys. Rev. Lett.* **99,** 153901 (2007).
124. Zhao, Q. *et al.* Electrically tunable negative permeability metamaterials based on nematic liquid crystals. *Appl. Phys. Lett.* **90,** 011112 (2007).
125. Hand, T. H. & Cummer, S. A. Frequency tunable electromagnetic metamaterial using ferroelectric loaded split rings. *J. Appl. Phys.* **103,** 066105 (2008).
126. Lim, S., Caloz, C. & Itoh, T. Metamaterial-based electronically controlled transmission-line structure as a novel leaky-wave antenna with tunable radiation angle and beamwidth. *IEEE Trans. Microwave Theory.* **53,** 161–173 (2005).
127. Chen, H. T. *et al.* Experimental demonstration of frequency-agile terahertz metamaterials. *Nature Photon.* **2,** 295–298 (2008).
128. Liu, S. *et al.* Manipulating negative-refractive behavior with a magnetic field. *Phys. Rev. Lett.* **101,** 157407 (2008).
129. Gao, Y. *et al.* Optical negative refraction in ferrofluids with magnetocontrollability. *Phys. Rev. Lett.* **104,** 034501 (2010).
130. Drachev, V. P. *et al.* The Ag dielectric function in plasmonic metamaterials. *Opt. Express* **16,** 1186–1195 (2008).
131. Blaber, M. G. *et al.* Plasmon absorption in nanospheres: A comparison of sodium, potassium, aluminium, silver and gold. *Physica B* **394,** 184–187 (2007).
132. Arnold, M. D. & Blaber, M. G. Optical performance and metallic absorption in nanoplasmonic systems. *Opt. Express* **17,** 3835–3847 (2009).
133. West, P. R. *et al.* Searching for better plasmonic materials. Preprint at <http://arxiv.org/abs/0911.2737> (2009).
134. Noginov, M. A. *et al.* Compensation of loss in propagating surface plasmon polariton by gain in adjacent dielectric medium. *Opt. Express* **16,** 1385–1392 (2008).
135. Fang, A. *et al.* Self-consistent calculation of metamaterials with gain. *Phys. Rev. B* **79,** 241104(R) (2009).
136. Popov, A. K. & Shalaev, V. M. Compensating losses in negative-index metamaterials by optical parametric amplification. *Opt. Lett.* **31,** 2169–2171 (2006).

Acknowledgements
This work was supported by Hong Kong RGC grant numbers HKUST3/06C and 600209. Computation resources were supported by the Shun Hing Education and Charity Fund.

Additional information
The authors declare no competing financial interests.